Supplementary Figures captions

Supplementary Table 1:
Brood sizes and hatch rates of *him-19(jf6)* selfed, outcrossed to wild-type males, or to *him-19(jf6)*males. Crosses of *fem-3* females to *him-19(jf6)* males show rather high hatch rates, suggesting that male meiosis is less affected than female meiosis.

	N2 co-supp	*him-19(jf6) self*	*him-19 (tm3538)*	*Him-19(jf6)fem* x N2 male	*him-19(jf6)fem* x *him-19(jf6)* male	*fem-3 x him-19 (jf6)* male68
Day 1	59.71% (n=432)	51.20% (n=334)	31.97% (n=926)	23.90% (n=88)	19.81% (n=429)	68% (n=367)
Day 2	38.89% (n= 563)	16.87% (n=1067)	14.91% (n=1522)	6.20% (n=129)	8.79% (n=182)	70% (n=333)
Day 3	25.0% (n=128)	4.34% (n=553)	3.27% (n=733)	0% (n=24)	7.5% (n=80)	88% (n=352%)
Day 4	22.22% (n=28)	6.43% (n=140)	n.a.	0% (n=14)	n.a.	93% (n=202)

Supplementary Figure 1.

him-19(tm3538) gonad organization.

A) DAPI stained *him-19(tm3538)* gonad. A defined TZ zone is missing in the mutant gonad.

B) *him-19(tm3538)* pachytene nuclei lack the parallel tracks observed in wild type pachytene nuclei.

C) Twelve univalents can be detected in the *him-19(tm3538)* mutants. Bars = 10μm

Supplementary Figure 2.

A) The protein meta-structure. Residue secondary structure and compactness plots of HIM-19a (A,B) and DHH-1 (C,D). The figure shows a comparison of predicted local secondary structural features (A,C) and compactness (B,D). Positive 2nd structure values are indicative of α-helical segments. In contrast, continuous negative values are typical for extended or β-strand regions. Large compactness values indicate residue positions typically buried in the interior of the 3D structure, whereas small values are found for residues exposed to the solvent.

B) Protein meta-structure alignment of HIM-19 and DHH-1. The pairwise protein sequence alignment is based on calculated meta-structure parameters. The scoring function for obtaining the optimal sequence match involves compactness and 2nd structure values. Black: pairwise alignment between HIM-19a and HIM-19b; Red: pairwise alignment between HIM-19a and DHH-1

Supplementary Figure 3.

Entry in meiosis is normal and uniform in *him-19* mutants. The chromosomal axes component HTP-3 localizes to chromosomes in cell rows 15 to 17 (excluding the distal tip cell) in both the mutant and wild-type. Left side shows DAPI images, HTP-3 staining and an overlay of entire gonads of both the wild type and the *him-19(jf6)* mutant. An enlargment of the distal end of the gonad is shown on the right. An arrowhead indicates cell rows 15 to 17, where uniform HTP-3 staining occurs. Bar=10µm

The inserted table shows for 5 independent wild-type and *him-19 (jf6)* worms in which cell rows HTP-3 staining can be observed along the chromosome axes. Spurious HTP-3 positive patches that are not associated with chromatin can also be observed more distally. Therefore, only cell rows in which more than two nuclei showed HTP-3 tracks along the chromosomes were considered.

Supplementary Figure 4.

A) Radiation causes increased loading of RAD-51 foci in *him-19* mutants. Worms were irradiated 48 hrs post L4 and stained for RAD-51 foci 1.5 hrs after irradiation.

B) Even *chk-2* mutants are able to load RAD-51 after irradiation. RAD-51 foci (red) can be observed on projections of gonads 6hrs post irradiation. DNA is stained with DAPI (blue). Bars = 10µm

Supplementary Figure 5.

A) SYP-1 associates between DAPI-positive structures both in wild type (N2) and *him-19(jf6)* meiosis. SYP-1 is stained in red and DNA in blue. Bar=10µm

B) Quantitative scoring of HIM-8 signals in association with SYP-1 stretches at the first five cell rows upon the start of SYP-1 loading. The categories were as follow: 1 (blue) unpaired HIM-8 signals with no association with SYP-1, 2 (purple) paired HIM-8 signals in association with SYP-1, 3 (yellow) unpaired HIM-8 signals in association with SYP-1, and 4 (turquoise) paired HIM-8 without association

with SYP-1. The category most often observed in wild type was the paired HIM-8 signals in association with SYP-1. In the *him-19(jf6)* background, the most frequent category was the unpaired HIM-8 signals in association with SYP-1. The association of HIM-8 and SYP-1 was random. Not all HIM-8 signals were associated with SYP-1 short stretches. Not all SYP-1 short stretches were associated with HIM-8. The SYP-1 polymerization seen at early pachytene could be associated with other chromosomes.

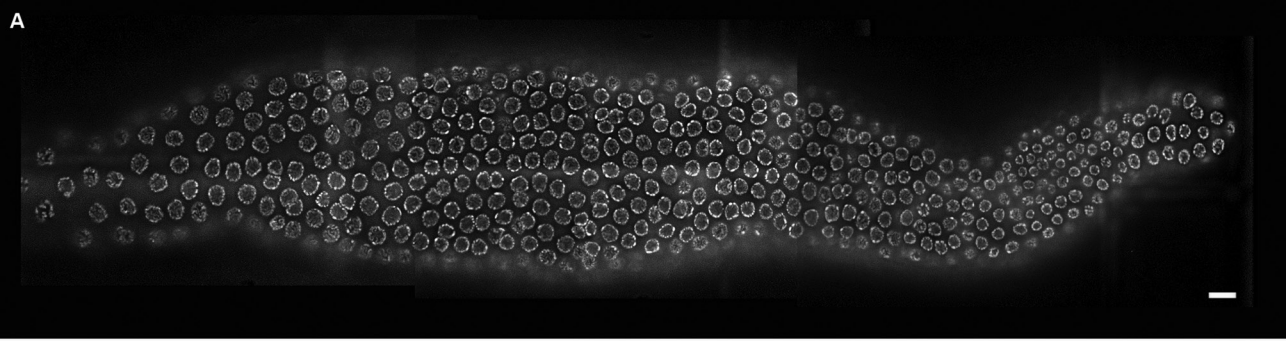

Tang et al., Supplementary Figure 1

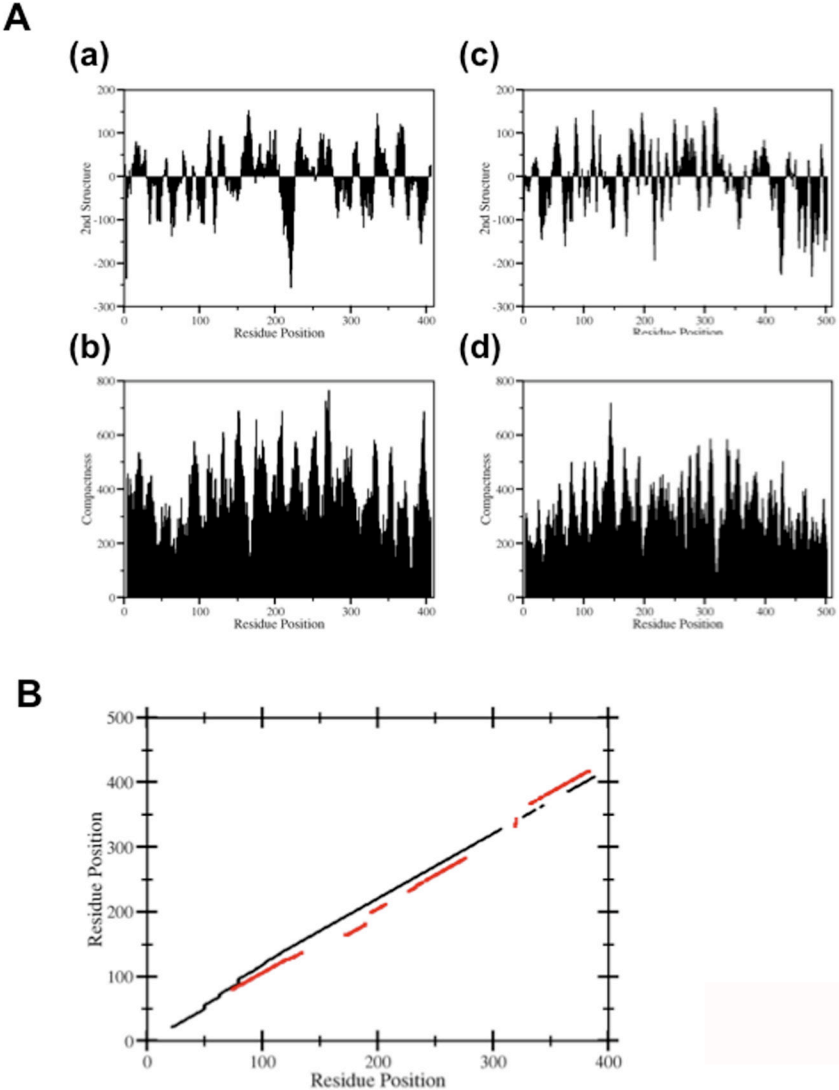

Tang et al., Supplementary Figure 2

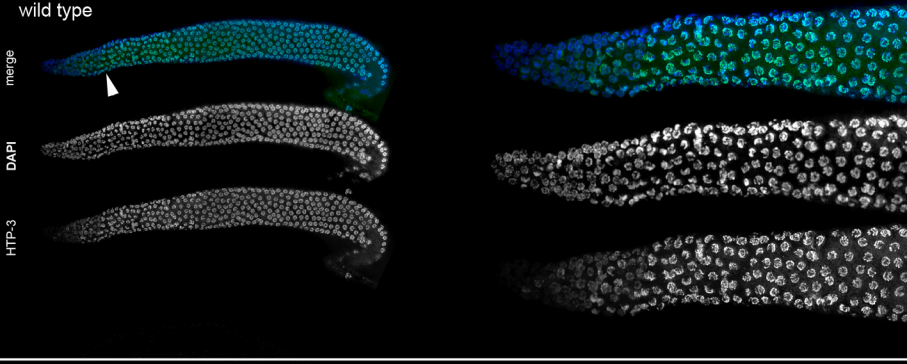

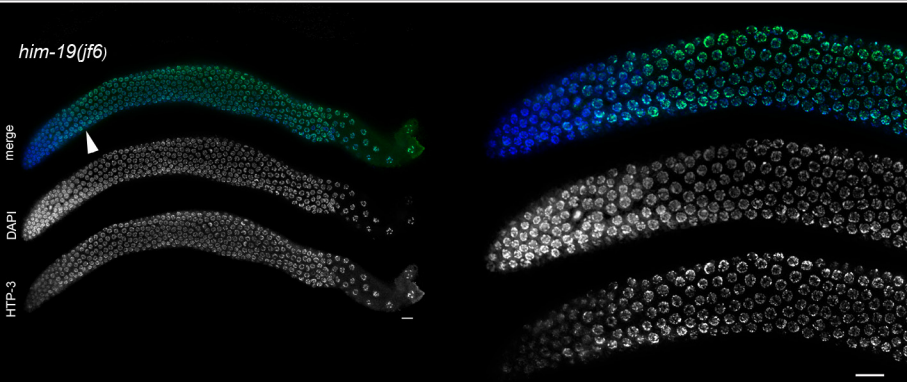

HTP-3 staining (Alexa 488) in 2-day old hermaphrodites

# of nuclear diameters (excl. DTC) distal to a zone containing >2 nuclei with chromatin-associated, linear HTP-3 structures

N2	
individuum #	nuclear diameter (excl. DTC)
1	16
2	15
3	18
4	15
5	17
average	**16,2**
S.D.	1,30

him-19(jf6)	
individuum #	nuclear diameter (excl. DTC)
1	17
2	12
3	16
4	17
5	17
average	**15,8**
S.D.	2,17

Tang et al., Supplemetary Figure 3

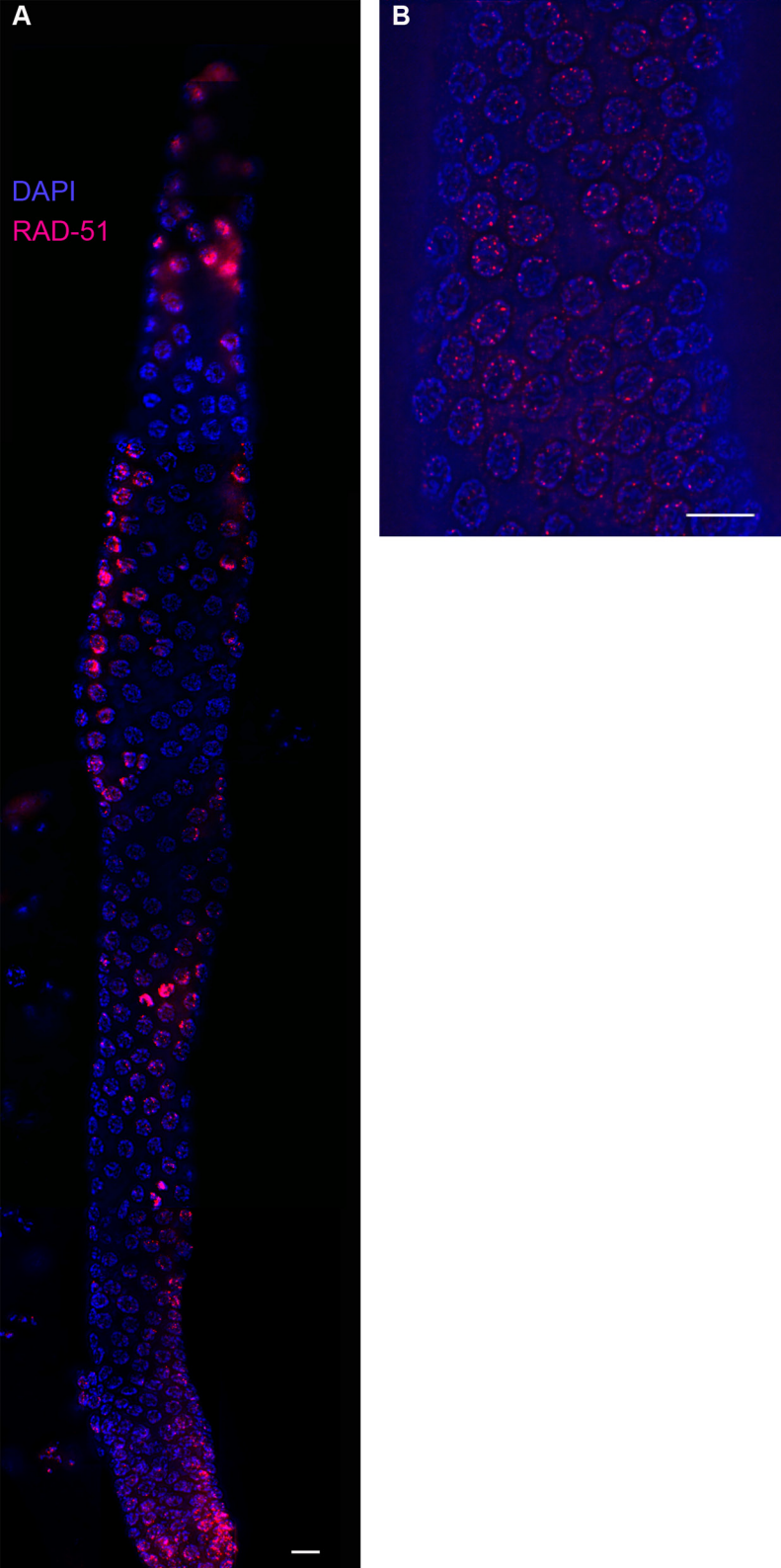
A
DAPI
RAD-51
B

Supplementary Figure 5.

A

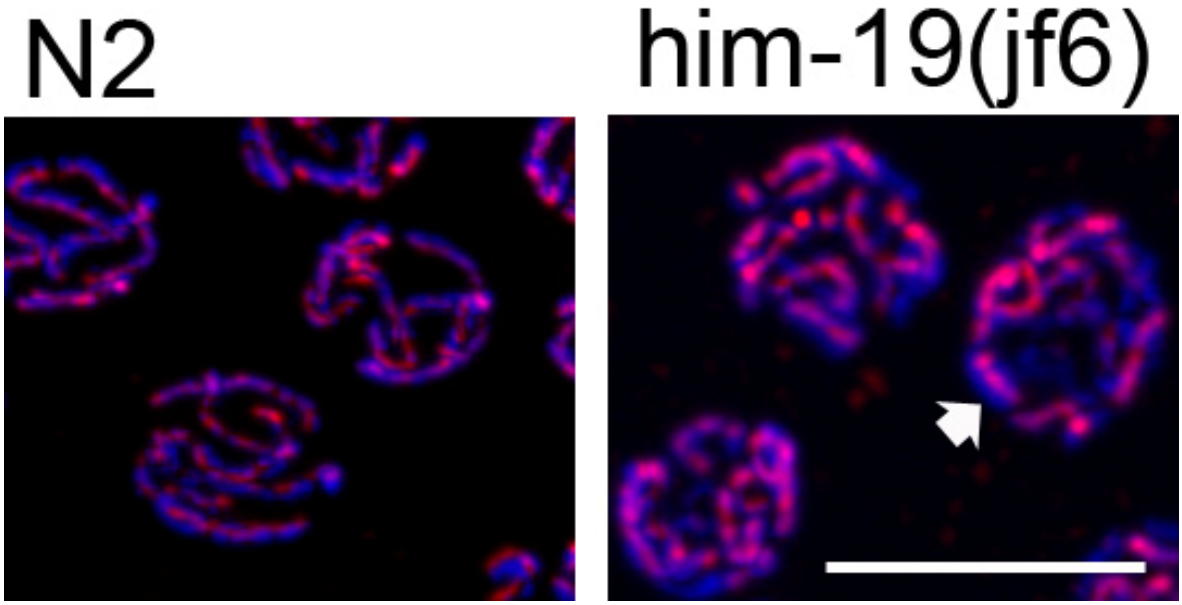

B

(N=56) (N=31)